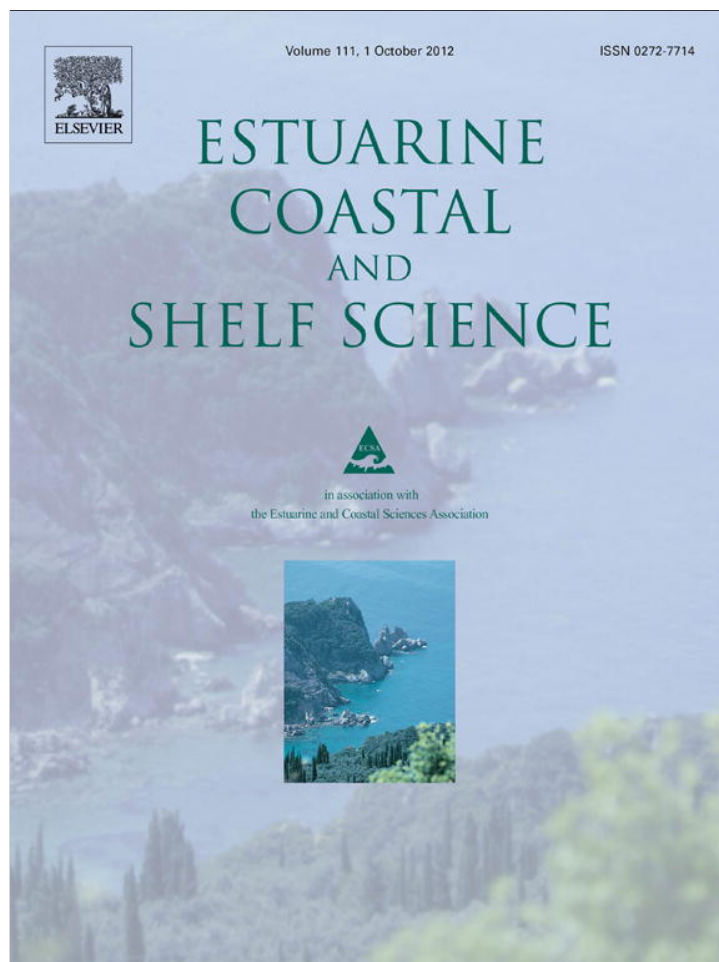


Provided for non-commercial research and education use.  
Not for reproduction, distribution or commercial use.



This article appeared in a journal published by Elsevier. The attached copy is furnished to the author for internal non-commercial research and education use, including for instruction at the authors institution and sharing with colleagues.

Other uses, including reproduction and distribution, or selling or licensing copies, or posting to personal, institutional or third party websites are prohibited.

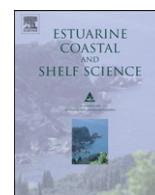
In most cases authors are permitted to post their version of the article (e.g. in Word or Tex form) to their personal website or institutional repository. Authors requiring further information regarding Elsevier's archiving and manuscript policies are encouraged to visit:

<http://www.elsevier.com/copyright>



Contents lists available at SciVerse ScienceDirect

## Estuarine, Coastal and Shelf Science

journal homepage: [www.elsevier.com/locate/ecss](http://www.elsevier.com/locate/ecss)

# The ENSO signature and other hydrological characteristics in Patos and adjacent coastal lagoons, south-eastern Brazil

Andrea I. Pasquini<sup>a,\*</sup>, Luis F.H. Niencheski<sup>b</sup>, Pedro J. Depetris<sup>a</sup>

<sup>a</sup> Centro de Investigaciones en Ciencias de la Tierra, CICTERRA (CONICET-UNC), Avenida Vélez Sarsfield 1611, X5016GCA Córdoba, Argentina

<sup>b</sup> Fundação Universidade Federal do Rio Grande (FURG), Depto. de Química, Laboratório de Hidroquímica, CP 474, CEP 96201-900, Brazil

## ARTICLE INFO

### Article history:

Received 31 October 2011

Accepted 8 July 2012

Available online 15 July 2012

### Keywords:

trend analysis  
harmonic analysis  
coastal lagoon  
El Niño  
wavelets  
Patos Lagoon

## ABSTRACT

With a surface area of over 10,000 km<sup>2</sup>, Patos Lagoon is Brazil's largest (choked) coastal lagoon. Directly or indirectly, Patos is associated with two other coastal lagoons, Mirim and Mangueira. Patos Lagoon reaches maximum water level height during the austral winter, in coherence with the rainy season. The longest (1961–2011) available rainfall (recorded at nearby Porto Alegre, Southern Brazil) and river discharge time series (1940–2011, in the tributary Jacuí River, at Rio Pardo) shows an overall increasing trend through the application of Mann–Kendall analysis. If, however, the series are split in two segments, negative trends become evident for the 1990–2011 period; in both cases earlier data showed a positive trend until ~1989. Coherent with water inflow, the lagoon's water height level shows a seasonal Kendall's  $\tau$  coefficient that is consistently negative for the month of April (statistically significant  $p$ ). Rainfall over Patos' drainage basin is actively teleconnected with ENSO occurrences in the equatorial Pacific. This can be verified in Porto Alegre's rainfall as well as in the Jacuí River discharge time series and in the lagoon's water level variability; a distinctly negative Southern Oscillation Index (SOI) usually results in excess precipitation, high riverine discharge and, accordingly, above normal lagoon water level. The use of a method for harmonic analysis (Continuous Wavelet Transform or CWT) allows detecting decadal and inter-annual periodicities in the rainfall and discharge frequencies and in the lagoon's water level time series. Also, a change in the frequency pattern appears to have occurred in the late 1990s (i.e., simultaneous with the 1997 ENSO event?) and suggests that it may be connected with the trend change which resulted in the current negative slope observed in deseasonalized hydrological data and a fainter ENSO signal for the region.

© 2012 Elsevier Ltd. All rights reserved.

## 1. Introduction

Coastal lagoons are relatively shallow water bodies separated from the ocean by a sand barrier, usually oriented along the shore. The lagoon is connected to the ocean, often sporadically, by one or more constrained inlets (Kjerfve, 1994). The Patos Lagoon (Fig. 1, Lagoa dos Patos in Portuguese) is one of the major coastal lagoons in the world and the largest in South America. It has been intensively studied from different points of view: biological (e.g., Garcia et al., 2003; Martins et al., 2007; Gilmar et al., 2008; Möller et al., 2009), environmental (e.g., Niencheski et al., 1994; Niencheski and Baumgarten, 2000; Mirlean et al., 2003), hydrological (e.g., Fernandes et al., 2002; Niencheski et al., 2007), and

sedimentological (e.g., Calliari et al., 2009; Vinzon et al., 2009), among other fields of environmental knowledge.

South of Patos Lagoon there are other smaller coastal water bodies: Mirim, to which Patos Lagoon is connected through a channel, and Mangueira Lagoon, sporadically linked with Mirim. Patos and Mangueira lagoons are genetically similar but are different from a hydrological point of view: Patos is connected with the sea and receives a major riverine water input; Mangueira does not have tributaries and only has a blurry connection in its northern fringe with Mirim Lagoon. Although Mangueira is smaller than Patos and the available data series is significantly shorter, information on the former has been herein included for the sole purpose of illustrating two different coastal lagoons that coexist in the area.

The climate at the Patos Lagoon, the surrounding area, and the drainage basin supplying it with runoff is complex, and variably influenced by climatic mechanisms such as the El Niño–Southern Oscillation or ENSO (e.g., Fernandes et al., 2002), or the position of the South Atlantic Convergence Zone or SACZ (e.g., Carvalho et al., 2004).

\* Corresponding author.

E-mail addresses: [apasquini@efn.uncor.edu](mailto:apasquini@efn.uncor.edu), [apasquini@com.uncor.edu](mailto:apasquini@com.uncor.edu) (A.I. Pasquini), [felipeniencheski@furg.br](mailto:felipeniencheski@furg.br) (L.F.H. Niencheski), [pdepetris@efn.uncor.edu](mailto:pdepetris@efn.uncor.edu) (P.J. Depetris).

<sup>1</sup> Tel.: +54 0351 4344983.



**Fig. 1.** Image showing the Patos-Mirim-Mangueira coastal lagoon system and its main features. The location of some measuring stations mentioned in the text are indicated in the figure with white circles.

In this contribution we are examining the recent evolution of rainfall in nearby recording stations, the most important riverine contribution, and the resulting variability in the lagoons' water level, particularly concerning trends and the incidence of ENSO in the existing measurement record.

## 2. Data and methods

### 2.1. Geographical and climatic framework

A relict of the Holocene Postglacial Marine Transgression, the Patos-Mirim Lagoon system ( $\sim 32^{\circ}\text{S}$   $\sim 49^{\circ}\text{W}$ )—as well as its neighbor, Mangueira Lagoon—is located in south-eastern Brazil (Fig. 1), occupying a significant area along the coastal plain of Rio Grande do Sul. Patos Lagoon is one of the largest choked lagoons in the world,  $\sim 250$  km long and  $\sim 60$  km wide, covering an area of over  $10,000$  km<sup>2</sup>; it has a mean depth of  $\sim 6$  m. Choked lagoons have a single inlet-channel and are characterized by a small ratio of inlet-channel cross-sectional area to lagoon surface area (Kjerfve, 1986); in the case of Patos, the inlet channel is  $\sim 800$  m wide, near the city of Rio Grande (Fig. 1). In Patos' southern extreme, the Sao Gonçalo channel connects it with Mirim Lagoon. Mirim is on the border between Brazil and Uruguay; it is  $\sim 190$  km long and covers an area of  $\sim 4000$  km<sup>2</sup> (Fig. 1). Mangueira Lagoon is located south of Patos (Fig. 1); it is a long ( $\sim 90$  km), relatively narrow ( $\sim 7$  km), and shallow ( $\sim 2.5$  m mean depth), non-tidal fresh water body, connected with Mirim through a low, marshy area (Santos et al., 2008a). The approximate mean water volume stored in Mangueira is  $0.7 \cdot 10^9$  m<sup>3</sup>.

The Patos Lagoon's drainage basin area exceeds  $200,000$  km<sup>2</sup> (Garcia et al., 2003, and references therein). The Jacuí River, is the system's main fresh water supplier, has upper catchments in the

hills, east of Passo Fundo, and flows southward and eastward for 450 km, receiving the Taquari, Caí, Sinos, and Gravataí rivers near its mouth. There, at Porto Alegre, it forms the Guaíba River, a shallow estuary emptying into the north end of the Patos Lagoon. The mean fresh water discharge to Patos Lagoon is  $\sim 4000$  m<sup>3</sup>s<sup>-1</sup>,  $\sim 90\%$  of which is supplied by the Guaíba River (Kjerfve, 1986); high discharge occurs during the austral winter (June–August), for the duration of which fresh water practically replaces salt water and occupies the entire lagoon system, thus controlling the circulation, salinity distribution, and the lagoon's water levels.

The dominant wind patterns (predominantly NE–SW) contribute to the control of circulation; they mainly drive it during the dry season (Niencheski et al., 2007, and references therein). Tides of about 0.5 m have little effect on the water level or circulation within the lagoon; the impact of tides is limited to the inlet, near Rio Grande. However, winds and the fresh water input can result in seasonally significant up-set or down-set of water levels. Over most of the lagoon, its water level is usually 0.5 m or more above the water level of the Atlantic (Niencheski et al., 2007).

During some ENSO events, whose linkage with Patos' dynamics has been shown by several authors (e.g., Fernandes et al., 2002; Möller et al., 2009), runoff greatly exceeds the lagoon's mean outflow discharge, sometimes exceeding  $25,000$  m<sup>3</sup>s<sup>-1</sup>, which is approximately the mean discharge of the nearby Río de la Plata (i.e., about the added mean discharges of the Paraná and Uruguay rivers, Pasquini and Depetris, 2007). Simulation exercises performed with data collected for the 1998 El Niño event showed that lagoon circulation was strongly related to wind behavior. An amplified discharge regime at the top of the lagoon led to increased outflows at the inlet; the higher the discharge, the stronger the pressure gradient toward the ocean, and a longer period that was necessary for the system to switch the flow landwards (Fernandes et al., 2002).

A most important feature of the seasonal climate variability in South America is the occurrence of a monsoon-like system that during the southern summer extends southward from the tropical continental region (Vera et al., 2006). It relates the Inter Tropical Convergence Zone (ITCZ) with the SACZ by means of a low-level jet that starts in the northeastern part of South America, runs along the Andes and supplies moisture to southeastern South America. Other important climatic characteristics are the occurrence of ENSO events, controlling atmospheric precipitations and, therefore, the hydrology of major fluvial systems (e.g., Pasquini and Depetris, 2007, and references therein), and the periodic incursions of polar air outbreaks east of the Andes (e.g., Garreaud et al., 2009).

### 2.2. Data analysis

The rainfall data series of Porto Alegre was obtained from the European Climate Assessment and Database (<http://climexp.knmi.nl>). Rainfall data at Rio Grande was obtained from FURG's meteorological station; rainfall data at Arambaré is being recorded by Brazil's Agência Nacional de Águas (ANA, <http://www.ana.gov.br>). Water level gauge data at Patos and Jacuí River discharge series were also acquired from ANA; Mangueira's was collected by FURG's technical personnel.

The Mann–Kendall test—*a.k.a.* Kendall's Tau—was used to assess the significance of trends in data series (Mann, 1945; Kendall, 1975), and the test known as seasonal Kendall (Hirsch et al., 1982) was employed to examine monthly trends. Both tests are non-parametric tools used to detect monotone trends in time series (e.g., Burn and Hag Elnur, 2002; Yue et al., 2002). The seasonal Kendall test has been selected as one of the most robust techniques now available to detect and estimate linear trends in environmental data (Hess et al., 2001).

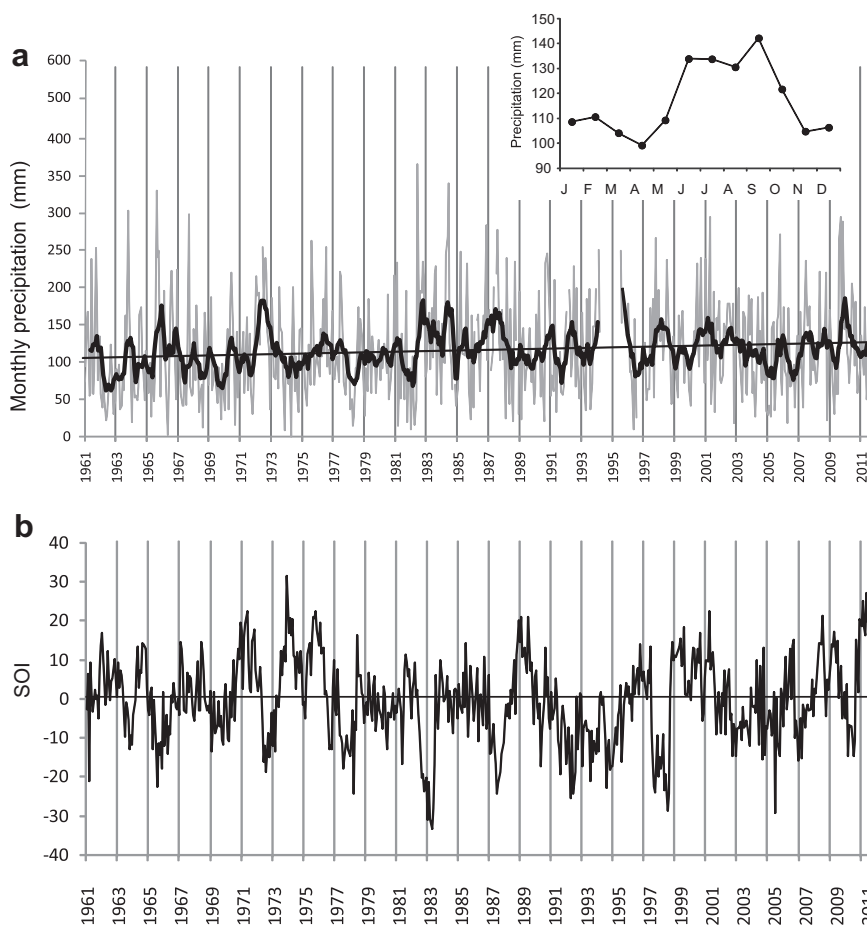


**Fig. 2.** a) Monthly precipitation time series at Porto Alegre for the 1961–2011 record period. Linear increasing trend is indicated ( $y = 0.041x + 104.6$ ;  $N = 581$ ). A 7-element moving average has been added. The mean annual pluviograph for the considered period is included as inset. Note that maximum precipitation occurs during austral winter and spring. b) Southern Oscillation Index (SOI) for the same period (<http://www.bom.gov.au/climate/current/soihtm1.shtml>).

In order to investigate periodicities in serial data, we have used deseasonalized monthly mean series obtained by subtracting the monthly historical means from monthly means. Data series are usually examined by either one of two spectral procedures: classical Fourier analysis or continuous wavelet transform (CWT). The classical Fourier transform does not contain any time dependence of the periodicity and uses sine and cosine base functions that have

infinite span and are globally uniform in time; it reveals what spectral component is present in the signal (Lau and Weng, 1995). The CWT, on the other hand, examines a time series using generalized local base functions (i.e., mother wavelets) that are stretched and decoded with a resolution in both frequency and time. This technique offers several advantages in comparison with traditional Fourier analysis because it supplies a time-scale localization for a signal. Thus, wavelet transform discloses some aspects that other spectral analyses miss, such as trends, breakdown points, and discontinuities (Nakkem, 1999). The literature offers numerous reviews on the theoretical aspects of CWT and Fourier analysis (e.g., Labat, 2005; Lau and Weng, 1995; Torrence and Compo, 1998).

### 3. Results and discussion

#### 3.1. Rainfall records in the area

To the best of our knowledge, the longest rainfall record (1961–2011) for the Patos Lagoon area is the one logged at Porto Alegre, Brazil (Fig. 1). Fig. 2 (inset) shows that atmospheric precipitation reaches a maximum during the austral winter and at the beginning of spring. The 50-year long Porto Alegre monthly rainfall time series (Fig. 2a) shows seasonality, the occurrence of extreme events and what appears to be a linear increasing trend. A comparison with the corresponding Southern Oscillation Index (SOI) (Fig. 2b) clearly shows that excess rainfall is frequently associated with strong El Niño events (i.e., markedly negative SOI).

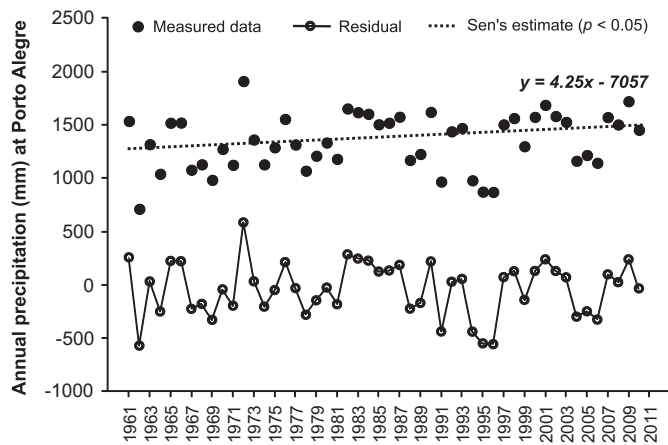


**Fig. 3.** Mann-Kendall test result for the mean annual precipitation at Porto Alegre (period 1961–2011). The increasing trend is statistically significant ( $p < 0.05$ ).

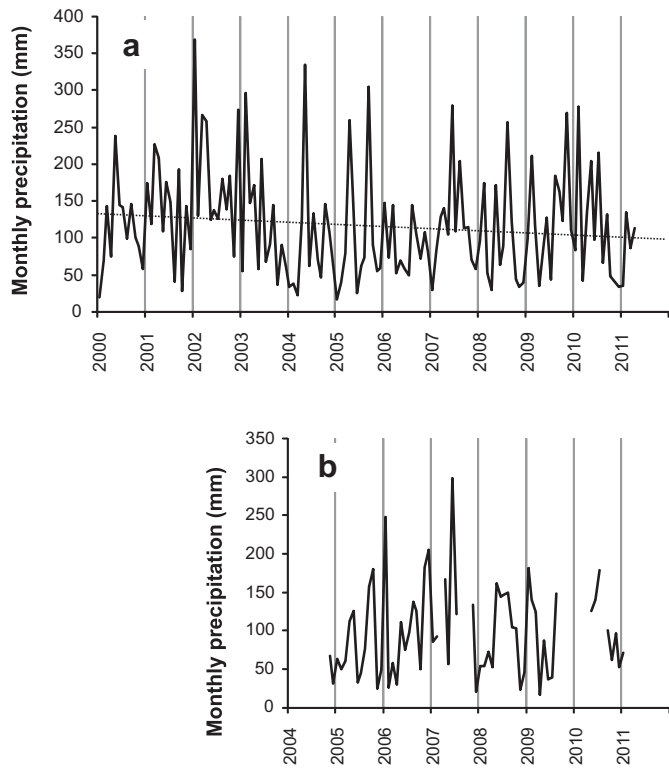


**Fig. 4.** a) Monthly precipitation series at Rio Grande (see location in Fig. 1) for the period 2000–2011. Linear decreasing trend is indicated ( $y = -0.248x + 135.5$ ;  $N = 136$ ). b) The same but for Arambaré for the period 2004–2011.

Conspicuous events, such as those of 1965, 1972 or 1982, for example, correlate with exceptionally high precipitation. In contrast, strong La Niña (i.e., positive SOI), like the one occurred in 1973, usually correlate with below-normal precipitation; the 2010 La Niña event was the strongest ever observed and the negative effect over precipitations in the region (i.e., SE South America) has been noticeable.

The Mann–Kendall test (Fig. 3) provides a statistical support to the linear positive trend of Fig. 2a: the slope indicates that, for the period 1961–2011, annual rainfall has been increasing at a mean rate of over 4 mm per year (Sen's estimate,  $p < 0.05$ ).

The inspection of shorter and recent rainfall time series, however, shows a somewhat different picture. Fig. 4a, b shows the monthly atmospheric precipitation record at Rio Grande

**Table 1**  
Seasonal Kendall test results for precipitation time series at Porto Alegre. Observe that the test was run for the whole series (i.e., 1961–2011) and for two periods: 1961–1989 and 1990–2011.  $N$ : number of observations. Numbers in bold and italics correspond to statistically significant values as indicated. The asterisks indicate different levels of statistical significance: \* $p < 0.05$ ; \*\* $p < 0.01$ ; \*\*\* $p < 0.001$ .

Month	Period 1961–2011			Period 1961–1989			Period 1990–2011		
	$N$	Kendall $\tau$	$p$ value	$N$	Kendall $\tau$	$p$ value	$N$	Kendall $\tau$	$p$ value
January	49	1.509	0.0657	29	1.050	0.1468	20	0.5518	0.2905
February	49	0.629	0.2645	28	-0.040	0.4842	21	-0.6649	0.2530
March	49	-0.707	0.2398	28	0.277	0.3910	21	-0.7868	0.2157
April	50	<b>2.543</b>	<b>0.0055**</b>	29	<b>3.096</b>	<b>0.0001***</b>	21	<b>-1.6910</b>	<b>0.0454*</b>
May	49	<b>2.233</b>	<b>0.0128*</b>	28	<b>2.213</b>	<b>0.0134*</b>	21	0.9365	0.1745
June	48	0.916	0.1800	28	1.185	0.1179	20	-0.2922	0.3851
July	49	1.440	0.0750	29	1.576	0.0575	20	-0.6168	0.2687
August	49	-0.500	0.3085	29	0.582	0.2804	20	1.4608	0.0720
September	48	0.738	0.2303	29	-0.413	0.3399	19	1.1202	0.1313
October	46	0.663	0.2537	28	-0.632	0.2636	18	-0.2651	0.3954
November	47	<b>1.816</b>	<b>0.0347*</b>	28	<b>2.331</b>	<b>0.0099**</b>	19	-0.2100	0.4168
December	48	0.587	0.2787	29	-0.657	0.2557	19	-0.8402	0.2004
All combined	581	<b>2.794</b>	<b>0.0026**</b>	342	<b>2.368</b>	<b>0.0089**</b>	239	-0.3827	0.3510

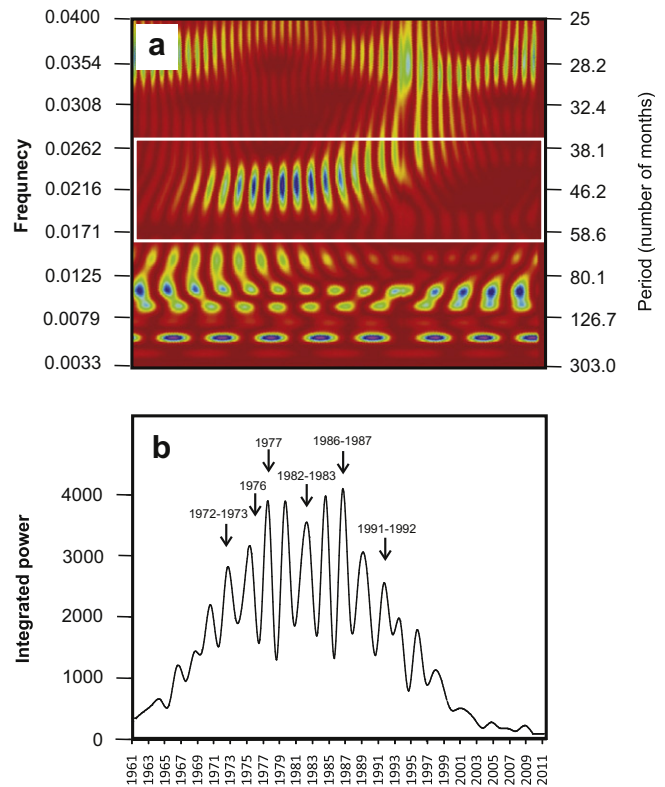


**Fig. 5.** a) Real part of the continuous Morlet wavelet spectrum for deseasonalized monthly precipitation time series at Porto Alegre. ENSO-like interannual periodical signal is framed. b) Wavelet power-frequency range for the ~40 to ~50 months frequency band for the same time series. El Niño years that match with high power are indicated with arrows. The increase in the signal power during the 70's and 80's is noteworthy.

(2000–2011) and Arambaré (2004–2011) (Fig. 1). These data series are relatively short and cannot be tested for trends by means of the Mann–Kendall technique to obtain a trustworthy result from a statistical point of view. However, the fitted linear regression line (Fig. 4a) shows a negative slope for the period 2000–2011. Moreover, some above- or below-average winter time rainfall at Rio Grande, for example, appear as coincidental with preceding ENSO phenomena (e.g., the 2002 and 2004 El Niño events, and the 2007 and 2010 La Niña events).

Therefore, the Porto Alegre rainfall data was analyzed by means of CWT, in order to search for periodic signals, discontinuities, and breakdown points in the time series. Fig. 5 shows the fifty-year long

(1961–2011) CWT spectra obtained from the deseasonalized rainfall time series at Porto Alegre. In Fig. 5a the signals with ENSO periodicity (~40 to ~60-month) have been framed. Fig. 5b shows the continuous Morlet wavelet power-frequency range (i.e., the total power for the highlighted area only), where it is clear the coherence with strong or intermediate ENSO events and, also, that the inter-annual signal has gathered power in the period that spans from early 1970s until early 1990s. Apparently, it has lost significance after that period, drifting the signal toward shorter periodicities and lesser significance. On the other hand, the decadal or quasi decadal signal has been consistent during the entire analyzed period.

On the basis of these results, the seasonal Kendall test was employed as the next step in the analysis. It allows the examination of the existence of a statistically significant trend in each month of the year. In the case of the monthly atmospheric precipitation series of Porto Alegre, it shows (Table 1) that the trend was significantly positive for April, May, and November during the last fifty years (i.e., for the period considered, atmospheric precipitations have been higher than the historical average during the three cited months). If, however, based on the image projected by the CWT analysis, one splits the rainfall series in two, and runs additional separate seasonal Kendall tests for 1961–1989 and 1990–2011, it turns out that during the twenty-eight years that span between 1961 and 1989, rainfall has been also increasing significantly in the months of April, May, and November (Table 1). Conversely, the period 1990–2011 reverses the trend and shows a negative and significant  $\tau$  coefficient for April, the month with the lowermost mean precipitation. Therefore, it is evident that the positive signature obtained for the fifty-year period is a consequence of the positive slope exhibited by the approximately first three decades of the series (i.e., 1961–1989): significant positive Kendall  $\tau$  coefficients are verifiable for the months of April, May, July and November (Table 1).

### 3.2. Jacuí River discharge variability at Rio Pardo

River discharge integrates rainfall over the expanse of drainage basins; therefore discharge series are good indicators of climate variability. This is the main justification for the inspection of the of Jacuí River time series at Rio Pardo gauging station (~100 km upstream from Porto Alegre, which is ~45 km from Patos Lagoon); it spans from 1940 until 2011 (Fig. 6a). The seasonal Kendall analysis for the whole deseasonalized series (Table 2) shows that there is a historical discharge increase during the low-flow months: January to May, November and December. If the series is split in two (as done before with the Porto Alegre rainfall series), the period 1940–1989 also exhibits an increasing trend for the lowermost flow months, just as the complete 1940–2011 series did. The 1990–2011 period, however, replicates the behavior seen in the similar (1990–2011) Porto Alegre rainfall series (Table 1). The trend analysis adds June to April, as the months showing a significant negative  $\tau$  coefficient. In other words, there is a significant decreasing trend in low-flow (April) and intermediate-flow (June) months.

Fig. 7a shows the CWT spectrum for the Jacuí River deseasonalized discharge series recorded at Rio Pardo. The ENSO-linked inter-annual periodicities are clearly discernible, as well as decadal and quasi-decadal signals. Fig. 7b shows the continuous Morlet wavelet power-frequency range (i.e., the total power for the framed area only), where the coherence with some ENSO events is apparent; the strong 1997–98 El Niño is especially outstanding. Probably due to differences in atmospheric circulation between the upper Jacuí River drainage basin and Porto Alegre (Fig. 5b), power appears somewhat shifted in the former (Fig. 7b).

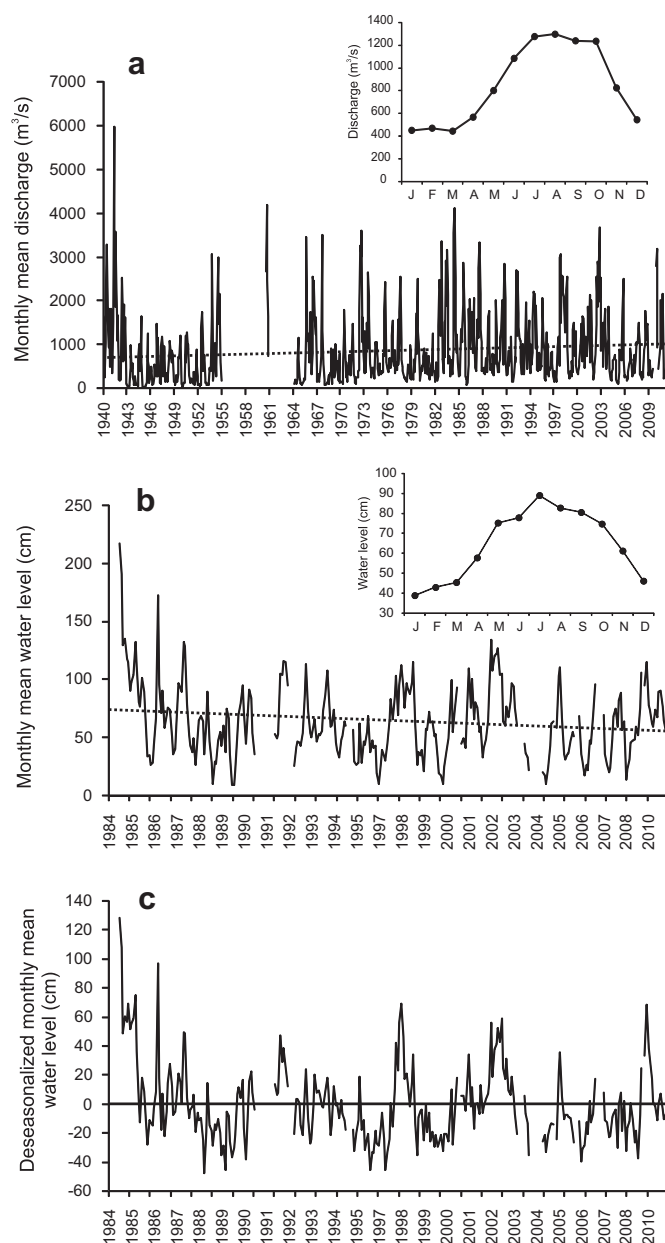


**Fig. 6.** a) Jacuí River discharge time series (1940–2010) at Rio Pardo; the mean hydrograph is included in the inset; the linear increasing trend is  $y = 0.379x + 680.2$ . b) Monthly mean water level time series in Patos Lagoon's for the period 1984–2010. Linear decreasing trend is indicated ( $y = -0.056x + 72.8$ ;  $N = 282$ ). Inset shows the historical annual hydrograph for the analyzed period. c) The same as b) but with deseasonalized data.

### 3.3. Water level variability at Patos and Mangueira lagoons

Gauge readings are available for the period 1984–2011 at the Patos Lagoon; the measuring gauge is located at Arambaré, at the lagoon's middle section (Fig. 1), ~70 km south of the Guaíba River's mouth. Fig. 6b (inset) shows the mean annual variation for the indicated time interval. The highest fresh water influx, through direct rainfall, riverine water supply, or groundwater seepage occurs during the austral winter. Therefore, the highest water levels are reached in July and the lowest in January (i.e., austral summer).

Fig. 6b shows the monthly mean water level variability (i.e., gauge readings) of the Patos Lagoon. Fig. 6c illustrates the same series, but deseasonalized. The seasonal Kendall test (Table 2)

**Table 2**  
Seasonal Kendall test results for Jacuí River discharge series [observe that the test was run for the whole series (i.e., 1940–2011) and for two separate periods: 1940–1989 and 1990–2011], and Patos Lagoon monthly mean water level time series at Aramaré (1984–2011). The asterisks indicate different levels of statistical significance: \* $p < 0.05$ ; \*\* $p < 0.01$ ; \*\*\* $p < 0.001$ .

Month	Jacuí river									Patos Lagoon		
	Period 1940–2011			Period 1940–1989			Period 1990–2011			Period 1984–2011		
	N	Kendall $\tau$	p value	N	Kendall $\tau$	p value	N	Kendall $\tau$	p value	N	Kendall $\tau$	p value
January	62	<b>1.7919</b>	<b>0.03658*</b>	40	1.1651	0.12199	22	-0.3666	0.35697	26	-0.639	0.26134
February	62	<b>2.6301</b>	<b>0.00427**</b>	40	<b>1.8409</b>	<b>0.03282*</b>	22	-1.4945	0.06752	25	-0.841	0.20024
March	62	<b>4.0150</b>	<b>0.00003***</b>	41	<b>3.2797</b>	<b>0.00052***</b>	21	-0.7247	0.23431	25	-0.724	0.23447
April	63	<b>3.4697</b>	<b>0.00026***</b>	41	<b>3.6167</b>	<b>0.00015***</b>	22	<b>-2.0584</b>	<b>0.01978*</b>	25	<b>-1.755</b>	<b>0.0379*</b>
May	63	<b>2.8410</b>	<b>0.00225**</b>	41	<b>2.5160</b>	<b>0.00593**</b>	22	-1.3253	0.09254	24	-1.588	0.05609
June	63	0.7770	0.21859	41	0.4043	0.34298	22	<b>-2.0021</b>	<b>0.02264*</b>	24	-0.868	0.19258
July	62	1.2573	0.10432	41	1.3928	0.08185	21	-1.1475	0.12559	21	-0.906	0.18249
August	62	0.8807	0.18923	42	1.6364	0.05087	20	0.2596	0.39760	23	-0.238	0.40606
September	62	1.3059	0.09579	42	1.4197	0.07785	20	0.8436	0.19946	22	0.423	0.33616
October	62	1.3545	0.08779	42	-0.6828	0.24738	20	0.5840	0.27961	21	-0.906	0.18249
November	62	<b>2.0956</b>	<b>0.01806*</b>	42	<b>2.4167</b>	<b>0.00783**</b>	20	0.1947	0.42283	22	0.028	0.48875
December	63	<b>2.2597</b>	<b>0.01192*</b>	42	<b>1.8749</b>	<b>0.03041*</b>	21	-0.4228	0.33624	24	-0.893	0.18594
All combined	748	<b>3.1960</b>	<b>0.00070***</b>	495	<b>2.6417</b>	<b>0.00412**</b>	253	-1.21205	0.11275	282	-1.273	0.10100

approximately follows the rainfall pattern for the same period: the Kendall  $\tau$  coefficient is negative for the month of April, with a statistically significant  $p$ . Since Patos Lagoon is not a closed basin (i.e., it has an inlet that connects it with the sea, where excess water drains out), there is a modulating effect that most likely attenuates the anomalies that the seasonal Kendall may have otherwise identified.

Mangueira Lagoon is located east of its neighbor, Mirim Lagoon (Fig. 1). It is a long and relatively narrow fresh water body, significantly smaller than Patos or Mirim lagoons, which appears influenced by groundwater seepage (Santos et al., 2008b). There is no direct linkage between Patos and Mangueira water bodies and,

therefore, water level gauge daily readings appear uncorrelated (Fig. 8a). The available data series –although too short to obtain statistically significant information– suggests that there is a lag in the water levels of Patos and Mangueira lagoons (i.e., maximum water levels in the latter are not reached in winter time). Moreover, the absence of a direct connection with the sea makes it prone to a seemingly harmonic signal (seasonal) in its water level time series (Fig. 8b). A comparison between Patos and Mangueira lagoons water height levels shows the occurrence of a lag (Fig. 8b), which may be associated with the chain-like morphology of the system: Patos is connected with Mirim, and Mirim is fuzzily linked with Mangueira. Moreover, Patos Lagoon is mostly fed by river flow and

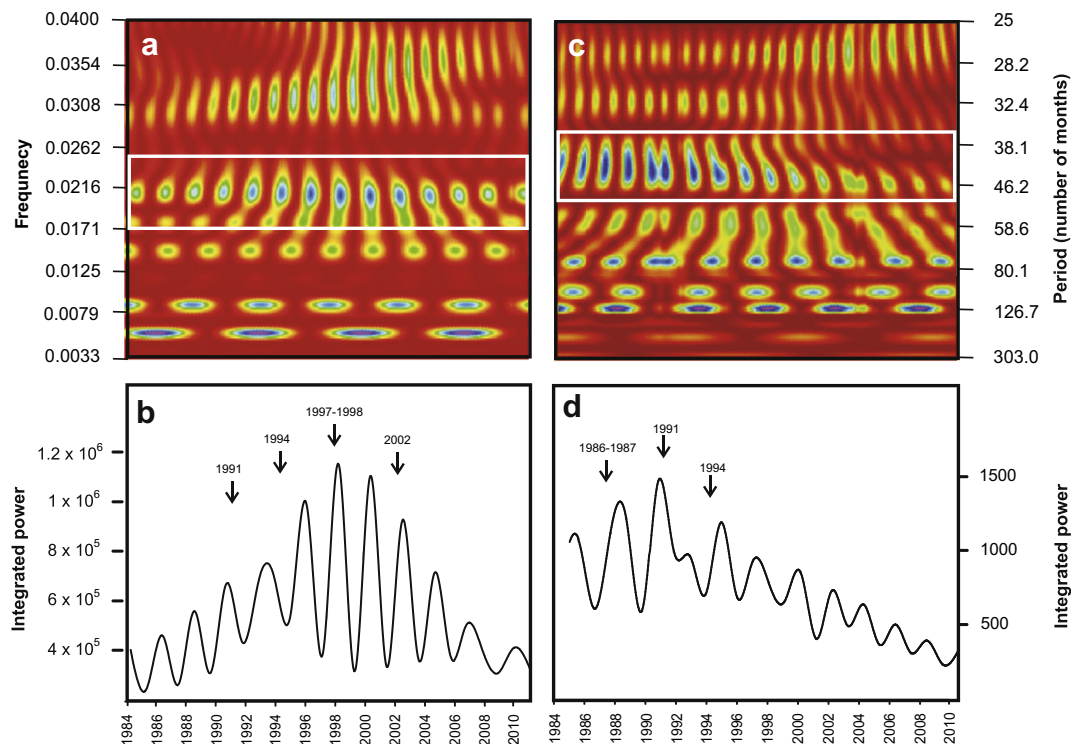


**Fig. 7.** a) Real part of the continuous Morlet wavelet spectrum for the Jacuí River discharge at Rio Pardo; the ENSO-determined periodicity has been framed. b) Frequency range power spectrum for the area framed in a); conspicuous ENSO events have been identified with arrows. c) Real part of the continuous Morlet wavelet spectrum for the Patos Lagoon monthly mean water level; ENSO-like inter-annual periodicity (~40 to ~50 months) is framed. d) Frequency range power spectrum for the 36–50 months frequency band for the same water level series. Some El Niño events occurred in this period are also indicated by arrows.

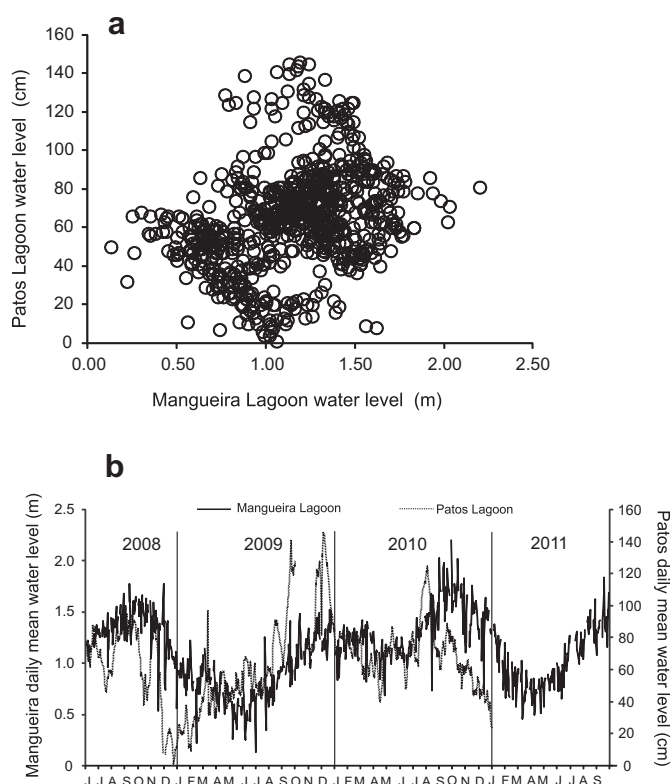


**Fig. 8.** a) Patos and Manguieira lagoons water level heights variability for the period 2008–2010; the absence of correlation is remarkable. b) Superimposed time series for Patos and Manguieira lagoons. Observe the variable lag between both series; Patos water level usually precedes Manguieira's.

has an inlet open to the sea whereas groundwater discharge seems to play a significant role in Manguieira.

Fig. 7c shows the CWT spectrum for the deseasonalized Patos Lagoon water level height time series (1984–2011); it displays decadal and inter-annual periodical signals, compatible with the hydrological effect determined by the occurrence of ENSO. Moreover, Fig. 7c also shows that decadal and quasi-decadal signals are persistent in the period whereas the inter-annual signal becomes fainter at the end of the 20th century and at the beginning of the 21st; it shows that, around 1998 the inter-annual signal (i.e., the framed area in Fig. 7c, ~40-month periodicity) which, up to that time seemed persistently regular, appears to fade away, while signals with lower periodicities become stronger. Fig. 7d illustrates the continuous Morlet wavelet power-frequency range of Patos Lagoon water height level series, where the occurrence of ENSO events (i.e., high integrated power) has been indicated. It is interesting to note the decreasing trend of integrated power after the end of the 20th century and, therefore, the decreased significance of ENSO.

#### 4. Conclusions

The hydrology of Patos and Manguieira lagoons is controlled by different systems: in Patos the effect of riverine fresh water supply and the sea water exchange mechanism are dominant, whereas in Manguieira, fresh water is mostly provided by groundwater and surface runoff. These diverse mechanisms result in an absence of correlation between both water height levels series and what appears to be a lag between the levels of both water bodies. A longer data series for Manguieira would be needed to reach definite conclusions. However, the possible existence of a lag suggests an

extended time-of-travel for groundwater and surface flow reaching Manguieira.

Many references in the scientific literature have shown that atmospheric precipitation is, ultimately, of utmost importance in the control of Patos Lagoon dynamics, influencing its chemistry, water level height, and circulation. The deseasonalized rainfall series at Porto Alegre shows a significantly positive trend in the fifty-year period that spans from 1961 until 2011. However, the statistical inspection of the Patos Lagoon deseasonalized water level height exhibits a faint but significant negative trend in April (for 1984–2011, the available period of gauge measurements which, interestingly, is the month with the lowermost mean rainfall in the region). This is the same trend that shows the deseasonalized rainfall at Porto Alegre (i.e., if a similar time period, 1990–2011, is chosen for the analysis). A break point has occurred along the time series, changing the trend from markedly positive to weakly negative. Strengthening the case, this phenomenon is also verifiable with the long discharge series recorded by Brazil's ANA for the Jacuí River, the most important fresh water source for Patos Lagoon.

CWT applied in both, the rainfall record at Porto Alegre and the water height level at Patos Lagoon (Figs. 5, 7 and 8), suggests that such inflexion point occurred in the mid- to late- 1990s, and may be somehow coincidental with the occurrence of the strong 1997 ENSO event which, as other similar events indicate, brought about excess rainfall to the region. The major difference between both CWT spectra is that the Patos Lagoon CWT spectrum (Fig. 7c) exhibits a ~70-month periodic signal (i.e., a likely harmonic of the ENSO signal) that is discernible during the 1990s and at the beginning of this century, which is absent in the Porto Alegre CWT rainfall spectrum (Fig. 5a). The signal of the inter-annual periodicities, compatible with ENSO-linked rainfall events in the region (~40-month), which starts fading at the end of the 20th century in the Porto Alegre rainfall series, and a bit earlier at the Patos Lagoon water level series, is the most interesting characteristic in this analysis. At any rate, there is a discernible change in those years after which, inter-annual periodicities faded away or exhibited an adjustment toward higher frequencies. At any rate, the change in trend in the riverine discharge and, therefore, in the lagoon's water height level appears connected with a decrease in El Niño intensity. This phenomenon leads to a simple but important question: did the ENSO signature become weaker in SE Brazil during the recent past?

#### Acknowledgments

This paper is a contribution to Project BR/09/05, framed within the CAPES (Brazil) – MINCYT (Argentina) scientific cooperation agreement. The authors would like to thank Carlos Andrade, Karina Attisano and Mariele Paiva for their help in gathering meteorological and hydrological data. This work was made possible by a grant from CNPq/Brazil (Grant 301985/09-0) to LFN. AIP and PJD acknowledge the support of Argentina's Consejo Nacional de Investigaciones Científicas y Técnicas (CONICET, PIP 11220080103160), and of the Universidad Nacional de Córdoba, Córdoba, Argentina. AIP and PJD are members of the CICYT in Argentina's CONICET.

#### References

- Burn, D.H., Hag Elnur, M.A., 2002. Detection of hydrologic trends and variability. *Journal of Hydrology* 255, 107–122.
- Calliari, L.J., Winterwerp, J.C., Fernandes, E., Cuchiara, D., Vinzon, S.B., Sperle, M., Holland, K.T., 2009. Fine grain sediment transport and deposition in the Patos Lagoon-Cassino beach sedimentary system. *Continental Shelf Research* 29, 515–529.



- Carvalho, L.M.V., Jones, C., Liebmann, B., 2004. The south Atlantic convergence zone: intensity, form, persistence, and relationships with intraseasonal to interannual activity and extreme rainfall. *Journal of Climate* 17, 88–108.
- Fernandes, E.H.L., Dyer, K.R., Möller, O.O., Niencheski, L.F., 2002. The Patos Lagoon hydrodynamics during an El Niño event (1998). *Continental Shelf Research* 22, 1699–1713.
- Garcia, A.M., Vieira, J.P., Winemiller, K.O., 2003. Effects of 1997–1998 El Niño on the dynamics of the shallow-water fish assemblage of the Patos Lagoon estuary (Brazil). *Estuarine, Coastal and Shelf Science* 57, 489–500.
- Garreaud, R.D., Vuille, M., Compagnucci, R., Marengo, J., 2009. Present-day South American climate. *Paleogeography, Palaeoclimatology, Paleoecology* 281, 180–195.
- Gilmar, A.F., Lemes, G.A.F., Kersanach, R., Pinto Lda, S., Dellagostin, O.A., Yunes, J.S., Matthiensen, A., 2008. Biodegradation of microcystins by aquatic *Burkholderia* sp. from a South Brazilian coastal lagoon. *Ecotoxicology and Environmental Safety* 69, 358–365.
- Hess, A., Iyer, H., Malm, W., 2001. Linear trend analysis: a comparison of methods. *Atmospheric Environment* 35, 5211–5222.
- Hirsch, R.M., Slack, J.R., Smith, R.A., 1982. Techniques of trend analysis for monthly water quality data. *Water Resources* 20, 107–121.
- Kendall, M.G., 1975. *Rank Correlation Methods*. Griffin, London, 202 pp.
- Kjerfve, B., 1986. Comparative oceanography of coastal lagoons. In: Wolfe, D.A. (Ed.), *Estuarine Variability*. Academic Press, Orlando, Fla, pp. 63–81.
- Kjerfve, B., 1994. *Coastal Lagoon Processes*. Elsevier Science B.V., Amsterdam, 577 pp.
- Labat, D., 2005. Recent advances in wavelet analyses: Part 1. A review of concepts. *Journal of Hydrology* 314, 275–288.
- Lau, K., Weng, H., 1995. Climate signal detection using wavelet transform: how to make a time series sing. *Bulletin American Meteorological Society* 76, 2391–2404.
- Mann, H.B., 1945. Nonparametric tests against trend. *Econometrica* 13, 245–259.
- Martins, I.M., Dias, J.M., Fernandes, E.H., Muelbert, J.H., 2007. Numerical modelling of fish eggs dispersion at the Patos Lagoon estuary – Brazil. *Journal of Marine Systems* 68, 537–555.
- Mirlean, N., Andrus, V.E., Baisch, P., 2003. Mercury pollution sources in sediments of Patos Lagoon estuary, southern Brazil. *Marine Pollution Bulletin* 46, 331–334.
- Möller, O.O., Castello, J.P., Vaz, A.C., 2009. The effect of river discharge and winds on the interannual variability of the pink shrimp *Farfantepenaeus paulensis* production in Patos Lagoon. *Estuaries and Coasts* 32, 787–796.
- Nakkem, M., 1999. Wavelet analysis of rainfall-runoff variability isolating climatic from anthropogenic patterns. *Environmental Modelling & Software* 14, 283–295.
- Niencheski, L.F., Baumgarten, M.G.Z., 2000. Distribution of particulate trace metal in the southern part of the Patos Lagoon estuary. *Aquatic Ecosystem Health and Management* 3, 515–520.
- Niencheski, L.F., Windom, H.L., Smith, R., 1994. Distribution of particulate trace metal in Patos Lagoon estuary (Brazil). *Marine Pollution Bulletin* 28, 96–102.
- Niencheski, L.F., Windom, H.L., Moore, W.S., Jahnke, R.A., 2007. Submarine groundwater discharge of nutrients to the ocean along a coastal lagoon barrier, Southern Brazil. *Marine Chemistry* 106, 546–561.
- Pasquini, A.I., Depetris, P.J., 2007. Discharge trends and flow dynamics of South American rivers draining the southern Atlantic seaboard: an overview. *Journal of Hydrology* 333, 385–399.
- Santos, I.R., Niensecki, F., Burnett, W., Peterson, R., Chanton, J., Andrade, C.F.F., Milani, I.B., Schmidt, A., Knoeller, K., 2008a. Tracing anthropogenically driven groundwater discharge into a coastal lagoon from southern Brazil. *Journal of Hydrology* 353, 275–293.
- Santos, I.R., Machado, M.I., Niencheski, L.F., Burnett, W., Milani, I.B., Andrade, C.F.F., Peterson, R.N., Chanton, J., Baisch, P., 2008b. Major ion chemistry in a freshwater coastal lagoon from southern Brazil (Mangueira Lagoon): influence of groundwater inputs. *Aquatic Geochemistry* 14, 133–146.
- Torrence, C., Compo, G.P., 1998. A practical guide to wavelet analysis. *Journal of American Meteorological Society* 79, 61–78.
- Vera, C., Higgins, W., Amador, J., Ambrizzi, T., Garreaud, R., Gochis, D., Gutzler, D., Lettenmaier, D., Marengo, J., Mechoso, C., Nogués-Paegle, J., Silva Díaz, P., Zhang, C., 2006. Towards a unified view of the American Monzón system. *Journal of Climate* 19, 4977–5000.
- Vinzon, S.B., Winterwerp, J.C., Nogueira, R., de Boer, G.J., 2009. Mud deposit formation on the open coast of the larger Patos Lagoon-Cassino Beach system. *Continental Shelf Research* 29, 572–588.
- Yue, S., Pilon, P., Cavadias, G., 2002. Power of the Mann–Kendall and Spearman' rho test to detecting monotonic trends in hydrological series. *Journal of Hydrology* 259, 254–271.